Canadian Mineralogist
Vol. 17, pp. 831-845 (1979)

SERPENTINIZATION OF THE BELVIDERE MOUNTAIN ULTRAMAFIC BODY, VERMONT: MASS BALANCE AND REACTION AT THE METASOMATIC FRONT*

THEODORE C. LABOTKA† AND ARDEN L. ALBEE
Division of Geological and Planetary Sciences, California Institute of Technology, Pasadena, California 91125, U.S.A.

ABSTRACT

Chrysotile-asbestos veins that cut the relatively unaltered dunite core of the ultramafic body at Belvidere Mountain, Vermont, are bordered by symmetrical serpentinite zones composed of antigorite, magnetite and brucite. This serpentinite is separated from the dunite host by a sharp reaction front, and the modal mineralogy and mineral chemistry of the two rock-types adjacent to the front were determined in order to characterize the serpentinization reaction. A mass balance of bulk chemistry indicates that the serpentinite formed by the addition of SiO_2 and H_2O, loss of H_2, and without net loss of magnesium. A reaction that most closely represents the serpentinization front is: 100 olivine + 25 SiO_2 + 129 H_2O = 31 antigorite + 4 magnetite + 4 H_2. The presence of essentially monomineralic zones suggests that SiO_2, H_2O and H_2 activities were externally controlled. Local concentrations of brucite indicate that the activities of those components were locally appropriate for the stability of brucite.

SOMMAIRE

Le noyau de dunite relativement fraîche du massif ultramafique de Belvidere Mountain (Vermont, USA) est recoupé par des filons d'asbeste-chrysotile bordés symétriquement de zones de serpentine. Un front de réaction sépare nettement de la dunite cette serpentine, composée d'antigorite, magnétite et brucite. Afin d'établir la réaction de serpentinisation, nous avons déterminé la minéralogie modale et la chimie des minéraux des deux types de roche en présence, de part et d'autre du front de réaction. Le bilan massique du chimisme global montre que la serpentine s'est formée par addition de SiO_2 et H_2O, avec perte de H_2, mais non de magnésium. La réaction 100 olivine + 25 SiO_2 + 129 H_2O = 31 antigorite + 4 magnétite + 4 H_2 représente au mieux la serpentinisation. Le caractère essentiellement monominéralique des zones fait penser que l'activité de SiO_2, H_2O et H_2 était réglée de l'extérieur, et des concentrations locales de brucite impliquent que cette activité favorisait localement la stabilité de la brucite.

(Traduit par la Rédaction)

INTRODUCTION

The ultramafic body at Belvidere Mountain, Vermont, has preserved a relatively unaltered dunite core within massive serpentinite. The dunite is cut by chrysotile veins that are symmetrically bordered by serpentinite zones. The sharp reaction-front between dunite and serpentinite was studied in order to characterize the physical-chemical nature of the serpentinization process.

Serpentinization has commonly been considered to occur either isovolumetrically or by simple hydration. Thayer (1966, 1967) suggested that the preservation of euhedral olivine pseudomorphs and relict primary chromite layering indicated volume-for-volume replacement of peridotite by serpentine, and that the excess MgO (and CaO) evolved during reaction may be deposited far from the serpentinite. Hostetler *et al.* (1966) considered that large-scale removal of MgO is unsupported by field evidence, and they, as well as Coleman & Keith (1971) and Page (1967a, b), argued that no significant amount of material is removed during serpentinization, that serpentinization occurs basically by hydration of the anhydrous peridotite assemblage, and that the large volume-change of the reaction is reflected by the abundant fractures and shear zones in serpentinites.

The Belvidere Mountain ultramafic body provides excellent examples of arrested serpentinization. The sharp metasomatic front near the chrysotile veins separates reactants (dunite) from products (serpentinite), and the determination of modal mineralogy, mineral distribution, mineral chemistry and bulk compositions con-

*Caltech contribution number 3165.

†Present address: Department of Earth and Space Sciences, State University of New York, Stony Brook, New York 11794, U.S.A.

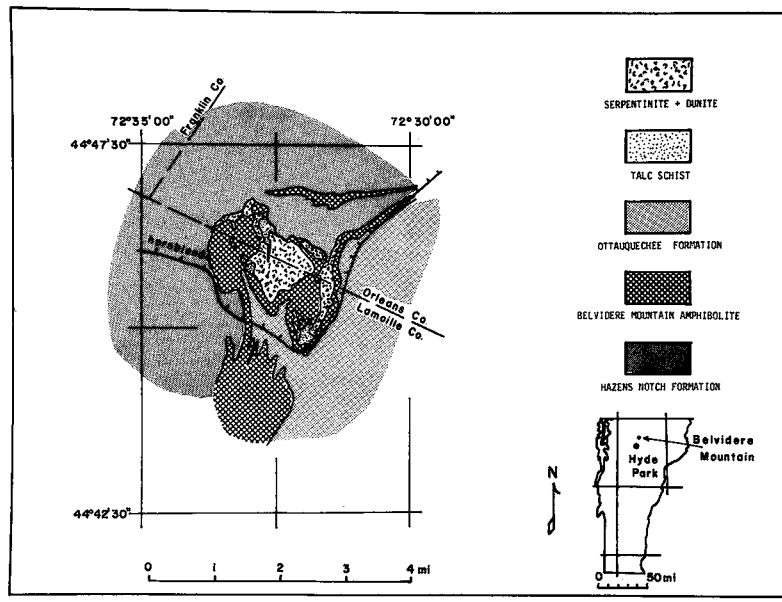

FIG. 1. Location and general geology of the Belvidere Mountain area, Vermont.

strains the type of reaction that may occur at the front.

GEOLOGY OF THE BELVIDERE MOUNTAIN AREA

The Belvidere Mountain ultramafic body, located in north-central Vermont, is one link in a north-trending chain of alpine-type ultramafic bodies that extends from Massachusetts into Québec (Cady *et al.* 1963, Chidester 1968, Chidester *et al.* 1978). The northern part of the chain occurs on the east limb of the Green Mountain anticlinorium, which in the Belvidere Mountain area comprises folded metasedimentary and metavolcanic rocks of Cambrian age. Figure 1 shows the general geology of Belvidere Mountain. The serpentinite was emplaced along the contact between a pelitic schist unit and an amphibolite unit in Late Ordovician (?) time; the margins of the serpentinite have developed local shear-zones that are foliated parallel to the contacts. The principal episode of folding and metamorphism occurred during the Devonian, but a record of an earlier folding and metamorphic event is preserved in the vicinity of Belvidere Mountain and Tillotsen Peak (Laird & Albee, in press). Wholesale serpentinization of the dunite probably occurred during emplacement, but at Belvidere Mountain a core of relatively unaltered dunite is preserved. During subsequent metamorphism, metasomatic alteration of the serpentinite occurred. At the margins of the serpentinite, zones of talc + magnesite and steatite were developed against a thin shell of chlorite schist (blackwall) at the contact with albite schist. Locally, the talc zones were not developed, and the country rock was altered to a serpentine–chlorite rock and calc-silicate rock (*i.e.*, rodingite: Chidester 1968). During metamorphism, cross-fibre chrysotile-asbestos veins developed in the ultramafic body, and where these veins cut relatively unaltered dunite, metasomatic zones of antigorite serpentinite occur between the chrysotile veins and dunite.

ANALYTICAL METHODS

Many of the chrysotile–serpentinite veins that cut dunite are less than 3 cm wide and may be covered by one thin section. Phase compositions were determined by electron-microprobe analysis with a MAC–5–SA3 automated microprobe. Operating conditions are 15 kV accelerating potential and 0.05 μa sample current on brass. Intensity data were reduced on-line using the technique of Bence & Albee (1968) and the correction factors of Albee & Ray (1970) with simple oxide and silicate standards. Precision was monitored by replicate analyses of well-characterized garnet and olivine and found to be ~2% for major elements and ~10% for

minor elements. H_2O was not directly determined, but is calculated by difference. Owing to the effect of the high OH content on the correction factors, the analyses for brucite have been normalized to the theoretical total for $Mg(OH)_2$.

Modal data were determined by optical point-count of three parts of the thin sections: dunite, the entire chrysotile vein plus the serpentinite zone, and the serpentinite zone within 2 mm of the reaction front. The mode of the serpentinite in ABM 1000 was determined by microprobe using automatic point-selection and phase identification by an energy-dispersive analyzer (Chodos *et al.* 1977). Representative analyses of phases in five samples are given in Tables 1 to 5. The modes and mineral compositions were used to calculate the bulk compositions of dunite and serpentinite for three samples.

Petrography

This study is based on five samples (AR–13f, ABM–1000, ABM–1001, ABM–1003, VAE–2) selected from the extensive collection used by Chidester *et al.* (1978) and which represent the textural varieties of chrysotile veins. The metasomatic serpentinite in these samples consists of a cross-fibre asbestos vein and a bordering serpentinite zone within the relatively unaltered dunite (Fig. 2). The central vein is a few millimetres wide and consists of chrysotile and magnetite. The fibre axis of chrysotile is oriented perpendicular to the walls of the vein and the chrysotile has an asbestos habit. The asbestos–magnetite vein is bordered by the serpentinite alteration-zone; the width of the serpentinite zone is symmetrical across the vein and ranges from less than 1 cm to several centimetres. In hand specimen the serpentinization front is knife-sharp, and the transition from the light green dunite to dark green serpentinite occurs over a distance of less than 1 mm. The dunite is generally structureless except that, in some samples, chromite grains form layers a few mm to a few cm wide.

The petrography and mineralogy of the dunite, the serpentinite front and the serpentinite zone are described below. In addition, sample VAE–2 is described separately because the characteristics of its reaction front are different from that in other samples.

Dunite

The dunite consists almost entirely of olivine

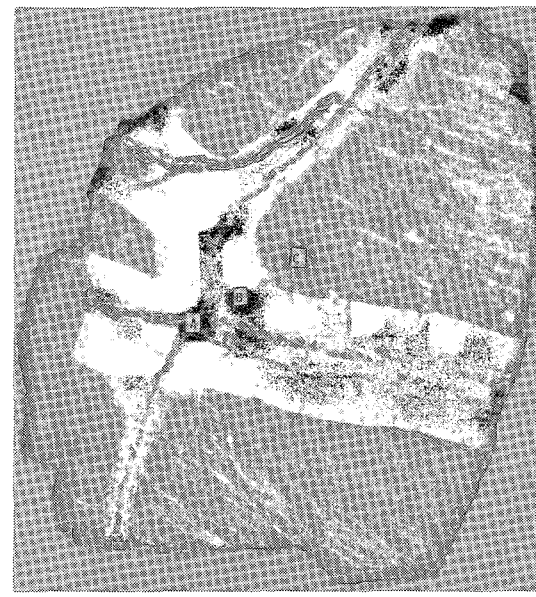

FIG. 2. Sample AR–13f showing cross-fibre chrysotile-asbestos vein (A), metasomatic serpentinite alteration-zone (B) and relatively unaltered dunite host (C). The maximum width of the sample is 15 cm.

in an equigranular, granoblastic fabric. The grains are approximately 0.5 mm in diameter and have straight boundaries in a polygonal aggregate. The composition of olivine ranges within the whole suite of samples from Fo_{91} to Fo_{95} (Tables 1 to 5), but olivine is unzoned and compositionally homogeneous within any one sample.

Pyroxene is absent in thin section, but a few irregularly shaped areas in ABM–1000 contain closely spaced, parallel magnetite lamellae that may be pseudomorphic after pyroxene schiller.

Chromian spinel and heazlewoodite (Ni_3S_2) are the only other primary phases in the dunite. Spinel generally occurs as large (2 to 4 mm) irregularly shaped grains concentrated into layers in ABM–1003, but dispersed in the other samples. The chromian spinel is in low abundance (<5%) in these samples, but chromite-rich bands do occur in the Belvidere Mountain body. The spinel contains a uniform chromium-rich (24 to 58% Cr_2O_3) core with up to 7% Al_2O_3. It has been partly altered along the rims and fractures to low-chromium (<1%) magnetite that contains no aluminum. Chromite that contains a relatively high amount of aluminum, *e.g.*, in VAE–2, also is surrounded by an outer zone

TABLE 1. REPRESENTATIVE PHASE COMPOSITIONS AND BULK COMPOSITIONS OF VAE-2

DUNITE

		Olivine	Chromite	Magnetite rim	Chlorite	Antigorite	Bulk[1]	Bulk[2]
Mode	(2000 pts)	89.2	1.9		6.9	2.0		
ρ		3.25	5.09		3.00	2.60		3.28
Wt. %		89.1	3.0		6.4	1.6	100.1	
	SiO_2	42.00	0.07	0.02	31.95	43.06	40.2	40.7
	TiO_2	0.00	0.02	0.00	0.01	0.01	0.0	0.0
	Al_2O_3	0.00	6.76	0.00	13.14	0.15	1.0	0.2
	Cr_2O_3	0.02	58.13	1.01	3.28	0.01	2.0	1.9
	MgO	52.00	6.64	1.03	35.43	43.25	49.5	50.6
	FeO^t	6.65	28.53	90.53	3.34	1.10	7.0	7.4
	MnO	0.03	0.46	0.60	0.03	0.06	0.0	0.0
	NiO	0.44	-	-	-	-		
	ZnO	-	0.31	0.00	0.00	0.00		
	F	-	-	-	0.10	0.23		
	Cl	-	-	-	0.00	0.02		
	H_2O	-	-	-	12.77	12.19	1.0	
	Total	101.15	100.92	93.24	100.00	100.00	100.7	100.8
	Mg/Mg+Fe	0.93			0.95	0.99		
	MgO/SiO_2						1.84	1.85

SERPENTINITE

		Antigorite	Chrysotile	Brucite	Magnetite	Chlorite	Chromite	Magnetite rim	Olivine relic	Bulk[3]
Mode	(3004 pts)	53.4	8.8	15.2	16.4	2.3	0.9		3.0	
ρ		2.60	2.60	2.39	5.20	3.00	5.09			2.95
Wt. %		47.1	7.8	12.3	28.9	2.3	1.6			100.0
	SiO_2	42.11	40.83	0.3	0.5	32.75	0.08	0.40		23.8
	TiO_2	0.00	0.00	0.0	0.00	0.01	0.02	0.00		0.0
	Al_2O_3	0.31	0.50	0.1	0.00	13.52	5.53	0.00		0.6
	Cr_2O_3	0.07	0.10	0.0	0.02	2.02	60.74	1.48		1.1
	MgO	43.27	43.22	67.0	0.87	35.97	6.63	1.47		33.2
	FeO^t	0.98	2.37	2.0	93.11	3.08	28.05	89.50		28.3
	MnO	0.04	0.02	0.5	0.56	0.07	0.39	0.57		0.2
	NiO	-	-	-	-	-	-	-		
	ZnO	0.14	0.00	0.0	0.06	0.01	0.29	0.10		0.1
	F	0.05	0.14	-	-	0.00	-	-		
	Cl	0.02	0.01	-	-	0.02	-	-		
	H_2O	13.06	12.87	30.0	-	12.54	-	-		11.2
	Total	100.00	100.00	100.00	94.67	100.00	101.76	93.57		98.5
	Mg/Mg+Fe	0.99	0.97	0.98		0.95				
	MgO/SiO_2									2.08

ΔV[4]	1.69
ΔSiO_2[5]	- 2.9
ΔFeO^t	+ 23.4

[1] Bulk composition excluding magnetite rim.

[2] Bulk composition excluding magnetite rim, chlorite and antigorite.

[3] Serpentinite vein is ∿1 cm. wide and no distinction between reaction zone and whole vein is made. See text.

[4] $\Delta V \frac{\text{serpentine}}{\text{dunite}} = \frac{(\text{wt. \% MgO})_{dun}\ \rho_{dun}}{(\text{wt. \% MgO})_{serp}\ \rho_{serp}}$

[5] $\Delta C_i = (\text{wt. \% } C_i)_{serp} - \frac{(\text{wt. \% Ci})_{dun}\ \rho_{dun}}{\Delta V\ \rho_{serp}}$ (in units of grams/100 grams serpentinite)

[t] Total Fe as FeO

of aluminum-poor (12 to 18% Al_2O_3), chromium-rich (~3% Cr_2O_3) chlorite. Heazlewoodite contains 0.2–1.2 wt. % Co, 0.02–2.1% Fe and 0.1–0.4 % Mg.

Most samples of dunite show various degrees of grain-boundary alteration to serpentine and brucite. Of the samples represented in Tables 1 to 5, dunite in AR-13f (Table 2) is the most extensively altered, containing more than 20% antigorite. This grain-boundary alteration corrodes the equant olivine, but the remnant cores are clear. In ABM-1001 (Fig. 3) and several samples not represented in the tables, the olivine in dunite is densely and minutely fractured. The densely fractured olivine and minor brucite alteration along the fractures give

TABLE 2. REPRESENTATIVE PHASE COMPOSITIONS AND BULK COMPOSITIONS OF AR-13f

		DUNITE				
		Olivine	Antigorite	Chromite	Bulk[1]	Bulk[2]
Mode [1]	(500 pts)	76.4	21.4	2.2	100.0	
ρ		3.25	2.60	5.09		3.29
Wt. % [1]		78.8	17.7	3.5		
	SiO_2	41.53	43.61	0.96	40.5	40.2
	TiO_2	0.02	0.01	0.02	0.0	0.0
	Al_2O_3	0.02	0.24	0.38	0.1	0.0
	Cr_2O_3	0.01	-	23.93	0.8	0.8
	MgO	51.82	43.45	2.22	48.6	50.1
	FeO^t	7.02	0.89	57.98	7.7	8.8
	MnO	0.20	0.07	5.27	0.4	0.4
	NiO	-	-	-		
	ZnO	-	0.02	0.54	0.0	0.0
	F	-	0.00	-		
	Cl	-	0.01	-		
	H_2O	-	11.71	-	2.1	
	Total	100.65	100.00	91.29	100.2	100.3
	Mg/Mg+Fe	0.93	0.99			
	MgO/SiO_2				1.79	1.86

		SERPENTINITE						
		Antigorite	Chrysotile	Brucite[4]	Magnetite	Chromite	Bulk[1]	Bulk[3]
Mode [1]	(1000 pts)	72.9	13.2	4.9	7.9	1.1	100.0	
$_3$	(1000 pts)	97.5	0.0	0.2	1.8	0.5		100.0
ρ		2.60	2.60	2.39	5.20	5.09	2.82	2.66
Wt. % [1]		67.2	12.2	4.1	14.6	2.0	100.1	
$_3$		95.3		0.2	3.5	1.0		100.0
	SiO_2	41.78	41.31	4.0	0.27	0.26	33.3	39.8
	TiO_2	0.00	0.01	0.0	0.0	0.01	0.0	0.0
	Al_2O_3	0.43	0.63	0.0	0.00	0.00	0.4	0.4
	Cr_2O_3	-	-	-	0.07	17.02	0.4	0.2
	MgO	42.35	42.61	60.3	0.89	1.45	36.3	40.5
	FeO^t	1.30	1.35	2.4	87.45	69.81	15.3	5.0
	MnO	0.14	0.11	0.3	0.25	3.17	0.2	0.2
	NiO	-	-	-	-	-		
	ZnO	0.00	0.00	0.1	0.10	0.18	0.0	0.0
	F	0.00	0.00	0.0	-	-		
	Cl	0.03	0.03	0.0	-	-		
	H_2O	13.98	13.96	32.9	-	-	12.4	13.4
	Total	100.00	100.00	100.00	89.03	91.90	98.3	99.5
	Mg/Mg+Fe	0.98	0.98	0.98				
	MgO/SiO_2						1.62	1.52
	ΔV[5]	1.61	1.53					
	ΔSiO_2[6]	+4.4	+7.4					
	ΔFeO^t	+9.0	-2.1					

[1] Entire rock type. [2] Bulk composition excluding antigorite. [3] Within 2 mm of dunite-serpentinite interface. [t] Total Fe as FeO. [4] Mixture of brucite and serpentine.
[5] ΔV defined in Table 1. [6] ΔC_i defined in Table 1.

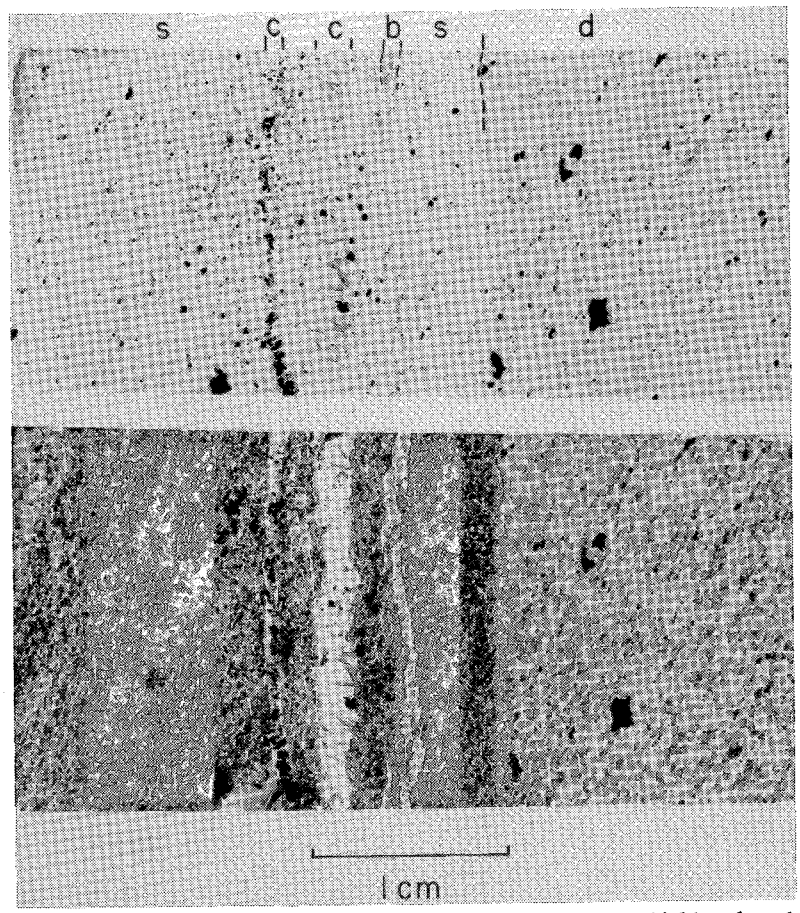

FIG. 3. Thin section of ABM–1001. Dunite (d) is more highly altered than either in ABM–1000 or VAE–2. There is no reaction zone present; of the two chrysotile veins (c), one has a high concentration of magnetite. A vein of brucite is conspicuous (b). Plane-polarized and cross-polarized light.

a cloudy or muddy appearance to olivine. The degree of grain-boundary alteration appears to have no direct correlation with distance from the serpentinization front, and this pervasive alteration of dunite probably occurred prior to development of the metasomatic front.

Serpentinite front

In all samples except VAE–2, the boundary between serpentinite and dunite is sharp to a scale of less than 1 mm. In some samples, such as ABM–1000 (Fig. 4), there is a narrow zone 1 to 5 olivine grains wide in which olivine is noticeably more fractured and altered to serpentine and brucite than the rest of the dunite. This reaction zone does not occur in most samples (*e.g.*, ABM–1001, Fig. 3) in which the degree of grain-boundary alteration in dunite is no greater near the serpentinization front than elsewhere in the dunite.

The serpentinite adjacent to the front consists almost entirely of antigorite with less than 5% brucite and magnetite (Tables 1–5, Figs. 3, 4). The grain size of antigorite is generally very small (<20 μm), and brucite and magnetite occur as 0.1 mm grains scattered in the serpentinite. Serpentine pseudomorphs after olivine are rare (except in VAE–2), and in general the serpentinite is structureless.

Serpentinite zone

The serpentinite zone consists of massive ser-

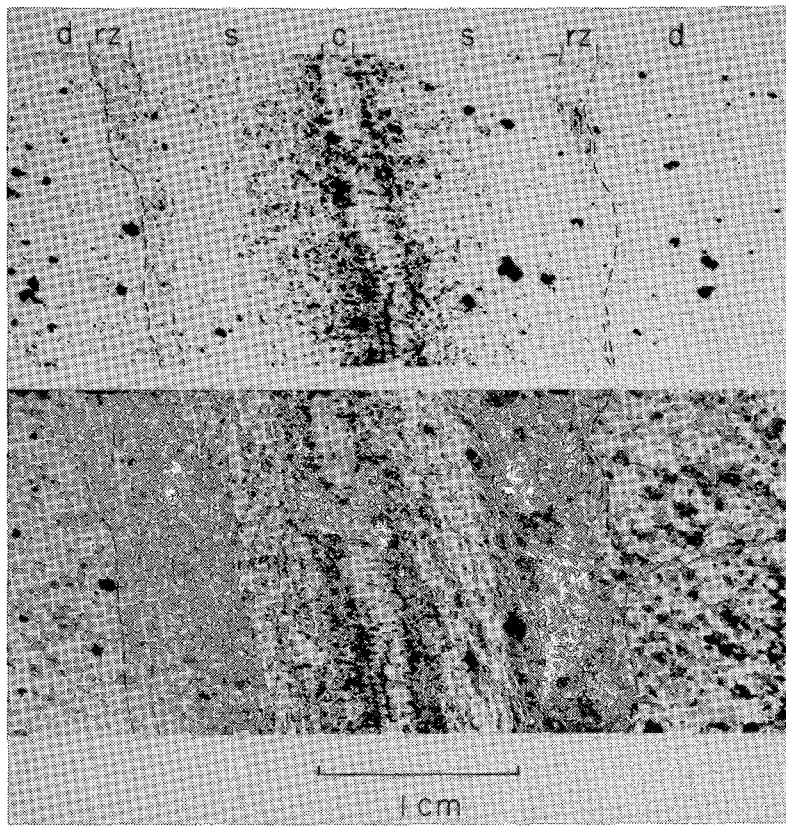

FIG. 4. Thin section of ABM–1000 showing chrysotile vein (c), metasomatic serpentinite (s), a narrow reaction-zone (rz) and relatively unaltered dunite (d). Chrysotile occurs in the serpentinite as light-colored streaks parallel to the vein. Large, irregularly shaped opaque grains are chromite, and small opaque grains are magnetite. Plane-polarized and cross-polarized light.

pentinite and veins of chrysotile asbestos and of brucite. The nonpseudomorphic, very fine-grained interpenetrating texture in the massive serpentinite and X-ray-diffraction patterns indicate that the serpentine mineral is antigorite (Wicks & Whittaker 1977). The composition of antigorite in VAE–2 is approximately $Mg_{5.97}Fe_{0.09}Al_{0.04}Si_{3.90}O_{10}(OH)_8$ (probe analysis normalized to Σ cations = 10), and ranges up to $Mg_{5.90}Fe_{0.14}Al_{0.14}Si_{3.81}O_{10}(OH)_8$ in ACM–1000 (Tables 1 to 5). Chrysotile occurs principally in the cross-fibre asbestos veins; however, in one sample (ABM–1000, Fig. 4), chrysotile, with its fibre axes oriented parallel to those in the vein, is also present in the serpentinite. The composition of chrysotile in the veins ranges from $Mg_{5.97}Fe_{0.18}Al_{0.06}Si_{3.78}O_{10}(OH)_8$ in VAE–2 to $Mg_{5.90}Fe_{0.12}Al_{0.08}Si_{3.89}O_{10}(OH)_8$ in ABM–1000. If serpentine is stoichiometric, most of the iron must be ferric in order to fill the tetrahedral sites. This assignment of ferric iron results in charge imbalance and suggests that serpentine is not stoichiometric. [Whittaker & Wicks (1970) argued that from a structural standpoint, antigorite must contain fewer than six filled octahedral sites *per* formula unit.] No pronounced or consistent differences in composition between antigorite and chrysotile are evident (*cf.*, Whittaker & Wicks 1970), and the textural evidence regarding the coexistence or co-occurrence of antigorite and chrysotile is ambiguous. In the Belvidere Mountain occurrence it is unclear whether chrysotile replaces antigorite polymorphically, or whether the two serpentine minerals coexist. Chrysotile does not occur at the serpentinization front; the serpentinization reaction is considered to involve antigorite with a stoichiometric composition.

TABLE 3. REPRESENTATIVE PHASE COMPOSITIONS AND BULK COMPOSITIONS OF ABM-1000

DUNITE

		Olivine	Chromite	Magnetite rim	Chlorite	Antigorite	Brucite	Bulk[1]	Bulk[2]
Mode [1]	(1000 pts)	88.7	4.6		6.2		0.6	100.0	
ρ		3.25	5.09			2.60	2.39		3.38
Wt. %		87.9	7.1		4.9			99.9	
	SiO_2	41.42	0.34	0.15	27.49	42.64		38.5	38.3
	TiO_2	0.00	0.05	0.01	0.02	0.01		0.0	0.0
	Al_2O_3	0.00	1.84	0.00	17.90	0.37		0.1	0.1
	Cr_2O_3	0.00	28.80	1.01	-	0.09		2.0	2.2
	MgO	50.56	3.04	1.06	35.18	42.72		46.8	47.0
	FeO^t	8.66	60.97	89.44	3.77	1.86		12.0	12.6
	MnO	0.07	2.71	0.27	0.28	0.09		0.3	0.3
	NiO	0.34	-	-	-	-			
	ZnO	-	0.55	0.04	0.00	0.06			
	F	-	-	-	0.05	0.00			
	Cl	-	-	-	0.05	0.02			
	H_2O	-	-	-	14.84	12.24		0.6	
	Total	101.05	98.30	91.98	100.00	100.00		100.3	100.5
	Mg/Mg+Fe	0.91			0.94	0.98			
	MgO/SiO_2							1.81	1.83

SERPENTINITE

		Antigorite	Chrysotile	Brucite[4]	Magnetite	Chromite[4]	Magnetite rim	Chlorite	Bulk[1]	Bulk[3]
Mode [1]	(4307 pts)		91.80	0.83	6.32	0.72			99.67	
Mode [3]	(1000 pts)	83.2	2.4	8.9	2.3		2.7	0.5		100.0
ρ		2.60	2.60	2.39	5.20	5.09			2.77	2.70
Wt. % [1]			86.1	0.7	11.9	1.3			100.0	
[3]		80.2	2.3	7.9	4.4	5.1				99.9
	SiO_2	41.25	41.96	0.3	0.11	0.34	0.05		35.5	34.1
	TiO_2	0.0	0.0	0.0	0.01	0.05	0.02		0.0	0.0
	Al_2O_3	1.01	0.69	0.0	0.00	1.84	0.00		0.9	0.9
	Cr_2O_3	0.38	0.08	0.0	0.4	28.80	3.16		0.7	1.8
	MgO	42.80	42.66	59.7	0.87	3.04	1.00		37.4	40.2
	FeO^t	1.76	1.43	6.2	92.16	60.97	90.26		13.3	9.1
	MnO	0.13	0.08	1.2	0.28	2.71	0.37		0.2	0.3
	NiO	-	-	-	-	-	-			
	ZnO	0.00	0.09	0.00	0.00	0.55	0.28			
	F	0.00	0.00	-	-	-	-			
	Cl	0.00	0.02	-	-	-	-			
	H_2O	12.64	12.98	32.6	-	-	-		11.1	13.0
	Total	100.00	100.00	100.00	93.47	98.30	95.17		99.1	99.4
	Mg/Mg+Fe	0.98	0.98	0.94						
	MgO/SiO_2								1.57	1.76

ΔV[5]	1.50	1.44
ΔSiO_2[6]	+ 4.8	+ 2.7
ΔFeO^t	+ 3.2	- 1.7

[1] Entire rock type. [2] Bulk composition excluding rim on chromite and hydrous minerals. [3] Within 2 mm of dunite-serpentinite interface. Chlorite and magnetite rim on chromite not included in bulk composition. [4] Values from analysis in dunite; satisfactory analysis from serpentinite not available. [5] ΔV defined in Table 1. [6] ΔC_i defined in Table 1. [t] Total Fe as FeO.

TABLE 4. REPRESENTATIVE PHASE COMPOSITIONS AND MODES OF ABM-1001

		Dunite					Serpentinite				
		Olivine	Antigorite	Chromite	Magnetite rim	Brucite	Antigorite	Chrysotile	Brucite	Magnetite	Chromite
Mode [1]	(1000 pts)	83.5	11.9		4.0	0.6	(1000 pts) 82.7	7.8	5.4	3.6	0.5
[2]	(1000 pts)						(1000 pts) 97.8	0.0	0.8	0.6	0.8
	SiO_2	41.95		0.10	0.07		42.49	42.08		0.15	
	TiO_2	0.00		0.02	0.01		0.00	0.02		0.01	
	Al_2O_3	0.00		0.12	0.00		1.16	1.43		0.00	
	Cr_2O_3	-		30.15	1.24		-	-		0.06	
	MgO	53.00		2.47	1.36		42.64	43.12		1.03	
	FeO[t]	4.91		62.85	88.70		2.11	2.62		90.94	
	MnO	0.34		3.11	0.12		0.15	0.06		0.06	
	NiO	-		-	-		-	-		-	
	ZnO	0.00		0.01	0.00		0.00	0.00		0.00	
	F	-		-	-		0.04	0.00		-	
	Cl	-		-	-		0.02	0.02		-	
	H_2O	-		-	-		11.40	10.65		-	
	Total	100.26		98.83	91.50		100.00	100.00		92.25	
	Mg/Mg+Fe	0.94					0.97	0.97			

[1] Entire rock type [2] Within 2 mm of dunite-serpentinite interface [t] Total Fe as FeO

TABLE 5. REPRESENTATIVE PHASE COMPOSITIONS AND MODE OF ABM-1003

		DUNITE								
		Olivine	Chromite	Magnetite rim	Chlorite	Antigorite	Chrysotile	Brucite	Heazlewoodite	Metal
Mode[1]	(1000 pts)	82.9	3.0		0.4	8.4	5.1	0.2		
	SiO_2	41.77	0.11	0.10	31.92	41.72	42.00	Mg	0.11	0.30
	TiO_2	0.03	0.05	0.02	0.00	0.00	0.01	Si	0.04	0.13
	Al_2O_3	0.00	4.67	0.00	12.42	0.14	1.52	P	0.00	0.00
	Cr_2O_3	0.04	51.31	0.79	n.d.	-	1.37	S	26.78	2.06
	MgO	52.09	5.42	0.96	34.05	39.54	40.13	Ca	0.00	0.01
	FeO[t]	6.15	36.09	89.03	3.53	1.09	2.57	Ti	0.00	0.00
	MnO	0.11	0.98	0.20	0.04	0.22	0.04	Cr	0.01	0.00
	NiO	-	-	-	-	-	-	Mn	0.00	0.00
	ZnO	-	0.42	0.00	0.03	0.04	0.03	Fe	0.02	19.03
	F	-	-	-	-	0.00	-	Co	0.32	1.28
	Cl	-	-	-	-	0.03	-	Ni	72.87	79.19
	H_2O	-	-	-	16.72[2]	16.00	12.34			
	Total	100.19	99.07	91.11	100.00	100.00	100.00		100.17	102.00
	Mg/Mg+Fe	0.94			0.95	0.98	0.96			

[1] Serpentine is concentrated along chromite seams [2] Value for H_2O includes Cr_2O_3 [t] Total Fe as FeO

Brucite occurs principally in veins in the serpentinite. A minor amount is interleaved with chrysotile in the cross-fibre asbestos vein, but the majority of brucite occurs in separate veins within the serpentinite. The vein brucite is fine grained and has a fibrous appearance with the long axis of the fibre oriented perpendicular to the vein. Brucite also occurs as individual, irregular grains within the serpentinite. This brucite makes up a small amount of the total serpentinite, but the grains are not evenly distributed and tend to occur in poorly defined layers that are parallel to the vein. The position of these brucite-rich layers relative to the serpentinization front is not constant. In ABM-1000 brucite is more abundant near the front (Table 3), and in AR-13f brucite is less abundant near the front (Table 2) than in the total serpentinite. Brucite has a composition ranging from $Mg_{0.94}Fe_{0.06}(OH)_2$ to $Mg_{0.98}Fe_{0.02}(OH)_2$.

Chromite relics are preserved in the serpentinite: these also contain magnetite rims and, in some cases, sheaths of chlorite. In many sections, chromite relics may be distinguished from secondary magnetite produced during serpentinization because chromite is much coarser and more irregular in shape (Fig. 4). Magnetite produced during serpentinization is generally euhedral or it forms aggregates of euhedral grains. This magnetite is concentrated in the

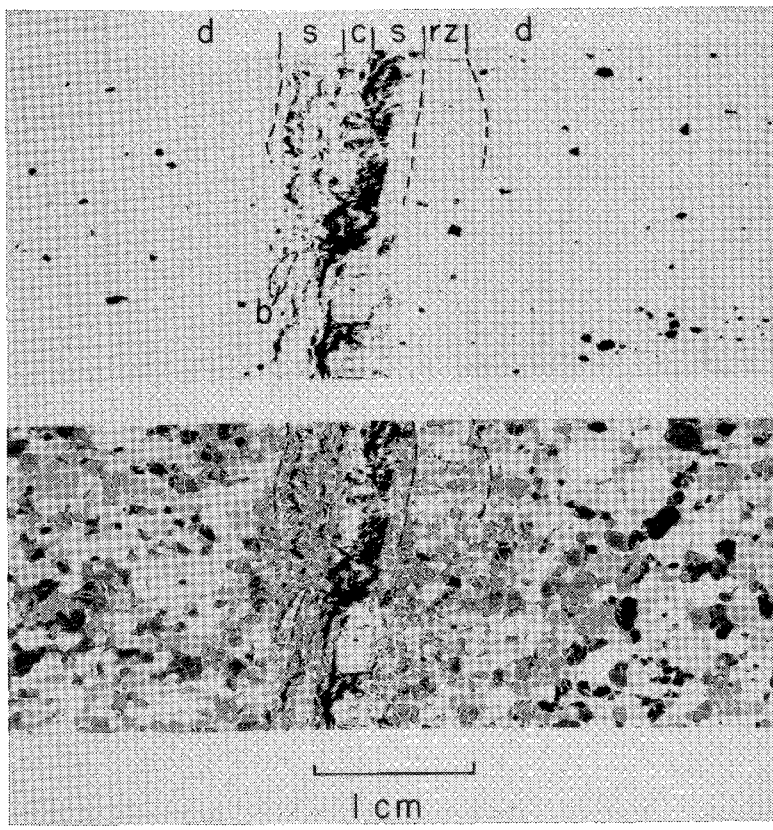

FIG. 5. Thin section of VAE–2. A wide reaction-zone (rz) is present, in which olivine is replaced pseudomorphically by antigorite and brucite. The reaction zone (rz) does not occur on the opposite side of the vein. Other features are as before: chrysotile vein with magnetite (c), brucite vein (b), serpentinite (s). Dunite (d) contains almost no grain-boundary alteration to serpentine.

cross-fibre asbestos veins and in the serpentinite immediately adjacent to them; in ABM–1000 the modal proportion of magnetite in the serpentinite visibly decreases away from the asbestos vein (Fig. 4). The composition of this secondary magnetite is distinct from the composition of magnetite on the rim of chromite; secondary magnetite contains no chromium and, generally, less magnesium than magnetite rims on chromite.

Metal grains occur in the veins; in specimen ABM–1003, they have the composition 79.2 wt. % Ni, 19.0% Fe, 1.3% Co, 2.1% S (Table 5).

VAE–2

The serpentinite in VAE–2 is texturally distinct from the other serpentinite alteration-zones described here. The reaction zone on one side of the chrysotile vein is characterized by abundant olivine relics that are pseudomorphically replaced by serpentine and brucite (Fig. 5). The pseudomorphic replacement of olivine and the abundant brucite are uncharacteristic of serpentinite in all other samples and of the serpentinization front on the opposite side of the chrysotile vein in VAE–2. At this front on the opposite side, the boundary between serpentinite and dunite is sharp, and brucite occurs principally in veins, similar to ABM–1001 and AR–13f. Because the serpentinite vein is relatively narrow and one of the reaction zones is wide, mass-balance calculations given in Table 1 are based on the mode of the entire serpentinite zone rather than on an attempt to separate serpentinite adjacent to the front from the rest of the serpentinite.

TABLE 6. POSSIBLE SERPENTINIZATION REACTIONS

	gm/Mole	ρ	Reaction I		Reaction II		Reaction III		Reaction IV		Reaction V	
			Moles	Vol%	Moles	Vol%	Moles	Vol%	Moles	Vol%	Moles	Vol%
Olivine[1]	144.8	3.25	100	100	100	99.9	100	100	100	99.9	100	100
Chromite[2]	206.4	5.09			0.08	0.1			0.05	0.1		
SiO_2			25.2		25.1							
H_2O			129.1		129.1		142.4		142.9		103.9	
CO_2											38.5	
Antigorite[3]	563.1	2.60	31.3	97.4	31.3	97.3	25.0	82.4	25.0	82.4	25.0	81.2
Brucite[4]	60.9	2.39					38.5	15.0	38.5	14.9		
Chlorite[5]	577.6	3.00			0.02	<0.1			0.01	<0.1		
Magnetite[6]	231.4	5.20	4.0	2.6			3.8	2.6			3.8	2.5
Magnetite[7]	229.4	5.20			4.2	2.6			4.0	2.7		
Magnesite[8]	89.3	2.98									38.5	16.3
H_2			4.0		4.1		3.8		4.3		3.8	
$\Delta O_{solid}(\% \Delta V_{solid})$	Products / Reactants		1.45		1.45		1.36		1.36		1.45	

I olivine + SiO_2 + H_2O = antigorite + magnetite + H_2
II olivine + chromite + SiO_2 + H_2O = antigorite + chlorite + magnetite + H_2
III olivine + H_2O = antigorite + brucite + magnetite + H_2
IV olivine + chromite + H_2O = antigorite + brucite + chlorite + magnetite + H_2
V olivine + H_2O + CO_2 = antigorite + magnesite + magnetite + H_2

[1] $Mg_{1.87}Fe_{0.13}SiO_4$ [2] $Mg_{0.35}Fe_{0.65}(Fe_{0.16}Cr_{1.56}Al_{0.28})O_4$ [3] $Mg_{5.97}Fe_{0.03}Si_4O_{10}(OH)_8$ [4] $Mg_{0.98}Fe_{0.02}(OH)_2$
[5] $Mg_{5.00}Fe_{0.26}Cr_{0.25}Al_{1.47}Si_{2.02}O_{10}(OH)_8$ [6] Fe_3O_4 [7] $Mg_{0.06}Fe_{2.91}Cr_{0.03}O_4$ [8] $MgCO_3$

Mass Balance

The modes of dunite, serpentinite adjacent to the reaction front and the entire serpentinite zone are given in Tables 1 to 5. The bulk composition of dunite was determined from the mode and mineral composition (Dunite Bulk[1] in the tables) and recalculated assuming that originally olivine and chromite composed the rock (Bulk[2] in the tables); that is, olivine and chromite are the reactants. The mode of the serpentinite adjacent to the reaction front is considered to represent the reaction products (Bulk[3] in Tables 2 and 3). The bulk composition of the entire serpentinite + asbestos vein (Serpentinite Bulk[1] in the tables) is also presented in order to compare compositions of the total mass of serpentinite to dunite.

Understanding the mass balance between dunite and serpentinite bulk-compositions is facilitated by comparing the actual modes in the two rock-types with the expected modes produced by possible serpentinization reactions. Table 6 lists several possible reactions using a single set of mineral compositions. The observed compositions of phases vary only slightly for different samples, and would cause only a small change in the stoichiometric coefficients. The reactions represent: (I and II) the addition of H_2O and SiO_2 to olivine to produce antigorite; (III and IV) the addition of H_2O only to produce antigorite and brucite, and (V) the addition of H_2O and CO_2 to produce antigorite and magnesite. Reaction I produces only antigorite and minor magnetite, whereas reaction III produces a rock with about 15 vol. % brucite. In all reactions about 2.5 vol. % magnetite is produced with a concomitant loss of H_2. Reactions II and IV illustrate the effect of chromite alteration on the predicted modes of antigorite and brucite. In both cases the effect of chromite is negligible, resulting in the appearance of small amounts of chlorite.

In no case do the predicted modes for serpentinite adjacent to the reaction front exactly match the observed modes. The mode of AR–13f (Table 2) most closely matches that predicted by reaction I, but brucite is present in the rock. The correspondence between the predicted and observed modes for the bulk serpentinite is characterized by an overabundance of magnetite and (except for VAE–2) a paucity of brucite in the rock. This imbalance between dunite (olivine) and serpentinite (antigorite + brucite + magnetite) is indicated in the MgO/SiO_2 values calculated for the three samples VAE–2, ABM–1000 and AR–13f (Tables 1, 2 and 3). With the exception of the unusual VAE–2, MgO/SiO_2 is lower in serpentinite than in dunite; hence, during hydration either magnesium was removed or silicon was added.

Within the entire, massive Belvidere Moun-

tain serpentinite, brucite is in very low abundance; Cady *et al.* (1963) estimated the abundance at less than 1 vol. %. Talc + magnesite and magnesite + quartz occur locally along the serpentinite but make up much less than 1% of the total serpentinite (Chidester 1968), and suggest a local high activity of CO_2 rather than a sink for excess MgO. Nowhere in the adjacent country-rock are there large deposits of brucite or magnesite that would provide evidence for large-scale transport of magnesium. The lack of identifiable magnesium sinks implies that silicon was added to the serpentinite. The country rock contains abundant quartz segregations and veins; it provides a logical source for SiO_2.

The Belvidere Mountain ultramafic body has undergone serpentinization with no apparent loss of MgO, and the mass balance between dunite and serpentinite is calculated on a MgO-con-

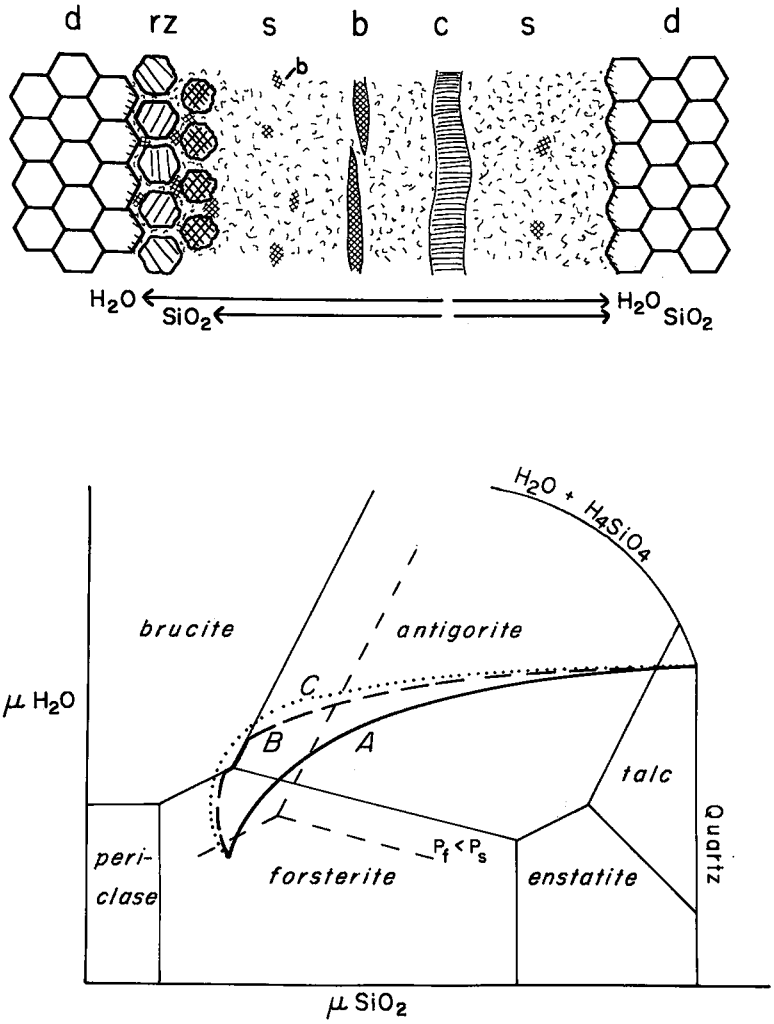

FIG. 6. (a) Idealized model for serpentinization at the metasomatic front with no reaction zone (right) and with a narrow reaction zone (left). Abbreviations as in Figure 5. (b) Possible diffusion-paths in terms of the chemical potentials of the independent components H_2O and SiO_2. The different possible diffusion-paths describe the three situations: (A) no reaction zone, (B) local equilibrium throughout a reaction zone, and (C) rate-controlled reaction zone.

servative basis. Note that in any mass-balance calculation, at least one relation between the two rocks (relative change in volume or in the concentration of a component) must be known. The difference in wt. % MgO between dunite and serpentinite reflects the difference in density and the change in volume due to the reaction. Tables 1 to 5 indicate the change in the amounts of SiO_2 and FeO^t (in units of grams/100 grams of serpentinite). In samples AR–13f and ABM–1000 (Tables 2 and 3) the indicated volume-increase is 1.45 to 1.60, and ~4.5% SiO_2 and several percent FeO^t must be added in order to balance the total serpentinite against dunite. The balance for VAE–2 (Table 1) indicates that nearly 3% SiO_2 must be removed. This inconsistency is probably an artifact of the difficulty in distinguishing brucite from finely intergrown antigorite in the wide reaction-zone.

Discussion

At Belvidere Mountain the formation of metasomatic serpentinite adjacent to chrysotile veins requires the addition of H_2O, SiO_2 and oxygen (loss of H_2). Reactions I and II (Table 6) most closely represent the serpentinization *front,* but brucite and magnetite are present in actual samples in excess of the amounts predicted by reactions I or II.

The wide zones of dunite and serpentinite are essentially monomineralic in phases that contain MgO + SiO_2 + H_2O, indicating that activities of two of the components may be externally controlled. The mass-balance arguments indicate that the solid-phase products are created by the addition of SiO_2 and H_2O to the solid-phase reactants without net loss of MgO. Hence, $\mu(MgO)$ may be considered determined by the externally controlled values of $\mu(SiO_2)$ and $\mu(H_2O)$. However, the presence of small amounts of brucite within the serpentinite indicates that locally only one of the three components may have had an independently determined chemical potential.

Figure 6a illustrates a qualitative model for wall-rock alteration in the Belvidere Mountain ultramafic body by multicomponent diffusion in the simplified system MgO–SiO_2–H_2O. The idealized rock contains unaltered dunite (d), a reaction zone (rz) that consists of fractured olivine with brucite and antigorite + brucite along grain boundaries, antigorite serpentinite (s) with local concentrations of brucite (b), a brucite vein (b) and a cross-fibre chrysotile-asbestos vein (c). Local equilibrium (Thompson 1959) is considered to exist everywhere except, perhaps, in the reaction zone. That is, reaction rates are faster than diffusion rates. Figure 6b illustrates an isothermal–isobaric $\mu(SiO_2)$–$\mu(H_2O)$ diagram for the boundary-value components SiO_2 and H_2O and possible diffusion paths for serpentinization. The driving forces for the advancement of the metasomatic front are (1) the differences in $\mu(SiO_2)$ and $\mu(H_2O)$ defined by the stability of forsterite in the dunite and (2) values defined by the quartz- and fluid-rich country rock. The boundary conditions on the diffusion path are fixed in dunite by "fluid" composition in equilibrium with olivine and in the country rock by a water-rich fluid in equilibrium with quartz. In part, the margin of the Belvidere Mountain serpentine consists of talc or talc + magnesite zones (Cady *et al.* 1963), and the fluid composition at the margin may be further constrained to be in equilibrium with quartz + talc and to be fixed at this composition so that no material leaves the serpentinite. This constraint provides for the change in bulk composition and the increase in volume during serpentinization. The actual diffusion path between the two boundary-conditions depends on the phenomenological coefficients for multicomponent diffusion (Cooper 1974) and on the nature of the rate-limiting process attending the reaction zone.

Path A corresponds to sharp reaction-fronts that show no zone of partly digested olivine. The serpentinization front represents values in $\mu(SiO_2)$ and $\mu(H_2O)$ [and, consequently, $\mu(MgO)$] appropriate for the equilibrium forsterite = antigorite. Path B describes component activities for serpentinization fronts with reaction zones (VAE–2 as the extreme example) if local equilibrium occurs in the reaction zone. The component activities must have the special values defined by the assemblages forsterite + brucite (muddy olivine), forsterite + brucite + antigorite (olivine grain-boundary) and antigorite + brucite (matrix of reaction zone). An alternative path, C, may represent the reaction zones if the reaction olivine → brucite is sluggish. The dunite side of the zone represents the equilibrium forsterite = brucite, but the incompletely digested olivine reflects a slow reaction rate. There is no gradual disappearance of olivine towards the serpentinite, and thus the serpentinite side of the reaction zone must represent the diffusion-controlled reaction brucite (+ relict olivine) = antigorite.

In all cases, the fluid that enters the fissure (chrysotile vein) has passed through a large volume of serpentinite and has a composition in equilibrium with antigorite. The rate of advancement of the serpentinite front depends on the rate of diffusion of SiO_2 and H_2O, so that

$$\frac{1}{a_{SiO_2}\, a_{H_2O}^{4}} = K_{eq}^{-1}$$

$$[\text{or } \mu_{antig} - (3\mu_{forst} + \mu_{SiO_2} + 4\mu_{H_2O}) = 0].$$

The increase in volume attending the reaction may result in production of new fractures and a local decrease in pressure on the fluid phase. Such a local drop in pressure may change the equilibrium constant so that brucite rather than antigorite is stable in the fractures. However, the local occurrence of brucite within the antigorite serpentinite would not be explained by this simple model. The small difference in Fe/Mg between antigorite and brucite does not seem sufficient to account for their coexistence, and fluctuations in fluid composition must have occurred so that the activities of SiO_2 and H_2O were locally buffered by the coexistence of brucite and antigorite.

Mass-balance considerations for the rocks at Belvidere Mountain indicate that material for additional magnetite was added to the total serpentinite + chrysotile vein, but that the amount of magnetite in the mode at the reaction boundary is similar to the amount predicted by reactions I or II. The serpentinization reaction produces a rock that is saturated with magnetite, and there is no apparent driving force for the addition of magnetite to serpentinite. Hydrogen is evolved at the serpentinization front, and a gradient in pH from a relatively low value at the front to a higher value in the fissure may play some role. The abundance of magnetite and the habit of the chrysotile must in some way be related to the physical properties associated with the presence of a vein (Chidester 1968).

The qualitative nature of the above discussion reflects the complexities of the details of the serpentinization process at Belvidere Mountain. The bulk compositions of dunite and serpentinite do place boundary conditions on this complex process. Serpentinization occurs with no net loss of magnesium from solid phases and with addition of H_2O and SiO_2 derived from the quartz-rich schist surrounding the serpentinite. Although brucite is present in small amounts, the reaction at the serpentinization *front* is closely approximated by olivine + SiO_2 + H_2O = antigorite + magnetite + H_2, a reaction which is neither isovolumetric nor "isochemical".

Acknowledgements

The perceptive review by F.J. Wicks is greatly appreciated. Support was provided by National Science Foundation grant EAR 75-03416.

References

Albee, A.L. & Ray, L. (1970): Correction factors for electron probe microanalysis of silicates, oxides, carbonates, phosphates, and sulfates. *Anal. Chem.* **42**, 1408-1414.

Bence, A.E. & Albee, A.L. (1968): Empirical correction factors for the electron-microanalysis of silicates and oxides. *J. Geol.* **76**, 382-403.

Cady, W.M., Albee, A.L. & Chidester, A.H. (1963): Bedrock geology and asbestos deposits of the upper Missisquoi Valley and vicinity, Vermont. *U. S. Geol. Surv. Bull.* **1122B**.

Chidester, A.H. (1968): Evolution of the ultramafic complexes of northwestern New England. *In* Studies of Appalachian Geology: Northern and Maritime (E-An Zen, W. S. White, J. B. Hadley and J. B. Thompson, Jr., eds.), Interscience, New York.

———, Albee, A.L. & Cady, W.M. (1978): Petrology, structure and genesis of the asbestos-bearing ultramafic rocks of the Belvidere Mountain area in Vermont. *U.S. Geol. Surv. Prof. Paper* **1016**.

Chodos, A.A., Albee, A.L. & Quick, J.E. (1977): The use of energy dispersive analysis for the study of phase aggregates. *12th Nat. Conf. Electron Probe Analysis* (Abstr.).

Coleman, R.G. & Keith, T.E. (1971): A chemical study of serpentinization – Burro Mountain, California. *J. Petrology* **12**, 311-328.

Cooper, A.R., Jr. (1974): Vector space treatment of multicomponent diffusion. *In* Geochemical Transport and Kinetics (A. W. Hofmann, B. J. Giletti, H. S. Yoder, Jr. & R. A. Yund, eds.). *Carnegie Inst. Wash. Publ.* **634**, 15-30.

Hostetler, P.B., Coleman, R.G., Mumpton, F.A. & Evans, B.W. (1966): Brucite in alpine serpentinites. *Amer. Mineral.* **51**, 75-98.

Laird, J. & Albee, A.L. (1980): High-pressure metamorphism in mafic schist from northern Vermont. *Amer. J. Sci.* (in press).

Page, N. J (1967a): Serpentinization at Burro Mountain, California. *Contr. Mineral. Petrology* **14**, 321-342.

——— (1967b): Serpentinization considered as a constant volume metasomatic process: a discussion. *Amer. Mineral.* **52**, 545-549.

THAYER, T.P. (1966): Serpentinization considered as a constant volume metasomatic process. *Amer. Mineral.* **51**, 685-710.

——— (1967): Serpentinization considered as a constant volume metasomatic process: a reply. *Amer. Mineral.* **52**, 549-553.

THOMPSON, J.B., JR. (1959): Local equilibrium in metasomatic processes. *In* Researches in Geochemistry (P. H. Abelson, ed.). John Wiley & Sons, New York.

WHITTAKER, E.J.W. & WICKS, F.J. (1970): Chemical differences among the serpentine "polymorphs": a discussion. *Amer. Mineral.* **55**, 1025-1047.

WICKS, F.J. & WHITTAKER, E.J.W. (1977): Serpentine textures and serpentinization. *Can. Mineral.* **15**, 459-488.

Received October 1978, revised manuscript accepted July 1979.